

Thierry A. G. M. Huisman

## Diffusion-weighted imaging: basic concepts and application in cerebral stroke and head trauma

Received: 12 June 2002  
Revised: 12 November 2002  
Accepted: 2 January 2003  
Published online: 6 March 2003  
© Springer-Verlag 2003

T. A. G. M. Huisman  
Department of Radiology,  
Neuroradiology Section  
and MGH–NMR Center,  
Massachusetts General Hospital  
and Harvard Medical School,  
Boston, MA 02129 USA

T. A. G. M. Huisman (✉)  
Department of Radiology,  
University Children's Hospital Zurich,  
Steinwiesstrasse 75, 8032 Zurich,  
Switzerland  
e-mail: [thierry.huisman@kispi.unizh.ch](mailto:thierry.huisman@kispi.unizh.ch)  
Tel.: +41-1-2667110  
Fax: +41-1-2667158

**Abstract** Diffusion-weighted imaging (DWI) of the brain represents a new imaging technique that extends imaging from depiction of neuro-anatomy to the level of function and physiology. DWI measures a fundamentally different physiological parameter compared with conventional MRI. Image contrast is related to differences in the diffusion rate of water molecules rather than to changes in total tissue water. DWI can reveal pathology in cases where conventional MRI remains unremarkable. DWI has proven to be highly sensitive in the early detection of acute cerebral ischemia and seems promising in the evaluation

of traumatic brain injury. DWI can differentiate between lesions with decreased and increased diffusion. In addition, full-tensor DWI can evaluate the microscopic architecture of the brain, in particular white matter tracts, by measuring the degree and spatial distribution of anisotropic diffusion within the brain. This article reviews the basic concepts of DWI and its application in cerebral ischemia and traumatic brain injury.

**Keywords** Diffusion-weighted imaging · Apparent diffusion coefficient · Fractional anisotropy · Cerebral ischemia · Traumatic brain injury

### Introduction

Diffusion-weighted magnetic resonance imaging (DWI) provides image contrast based on differences in diffusion of water molecules within the brain. Diffusion represents the random thermal movement of molecules, also known as Brownian motion. Diffusion within the brain is determined by a variety of factors including the type of molecule under investigation, the temperature and the micro-environmental architecture in which the diffusion takes place. For example, diffusion of molecules within the cerebrospinal fluid (CSF) is less limited than diffusion of molecules within the intra- and intercellular space. By using the appropriate magnetic resonance sequences that are sensitive for diffusion, these differences in diffusion rates can be used to produce image contrast. The first diffusion-weighted pulse sequences were described as early as 1965 by Stejskal and Tanner [1]. The demanding MR hard- and software requirements, however, delayed

the introduction as a clinical imaging technique for many years. It was not until the mid-1980s that diffusion-weighted imaging became available for clinical routine [2]. The recent development of high-performance gradients accelerated the use of DWI over the past few years. Meanwhile, quantitative maps that display the spatial distribution of the diffusion rate within the brain are generated within minutes.

Next to the magnitude of the diffusion rate, the direction of the strongest diffusion within three-dimensional (3D) space, which may differ between brain structures, can be displayed. The microstructural architecture as well as physiological factors influences the diffusion of water molecules within the brain. Within fiber tracts, the effective molecular diffusion is larger in the direction along the long axis of the fiber tract compared with the direction perpendicular to the fiber tract. This kind of diffusion is termed anisotropic diffusion in contrast to isotropic diffusion. In isotropic diffusion, the effective

diffusion is equal in all directions (e.g., CSF). The probable location of free movable water molecules will resemble a sphere, whereas the spatial distribution of water molecules within fiber tracts will resemble an ellipsoid or cigar after a time period. By measuring the full tensor of the diffusion, the 3D shape of diffusion can be measured. Maps of the spatial distribution and magnitude of the anisotropic component of diffusion can be generated. These maps provide information about the architecture and integrity of ordered tissues.

Multiple disease processes, including cerebral ischemia and traumatic brain injury, are characterized by changes in the rate and 3D shape of diffusion. In many cases, changes in the diffusion can be seen early, even before neurological symptoms become manifest or irreversible. Moreover, DWI allows the discrimination between lesions with increased and decreased diffusion. Many investigators believe that restricted water mobility is seen in lesions with cytotoxic edema, whereas increased water mobility is seen in lesions with vasogenic edema. Because cytotoxic edema is thought to occur early in brain ischemia, DWI is highly sensitive in the early detection of brain infarctions [3, 4, 5, 6]. As part of this early detection, DWI may provide important pathological–physiological information and might well give information about the possible reversibility of tissue injury. In addition, the early detection of signal changes, before conventional MR sequences show pathology, can be used to start treatment as early as possible [3, 4, 5, 6]. Because “time is brain,” early diagnosis with early treatment is expected to improve outcome. In addition, information about changes in the degree of anisotropic diffusion could give early information about the disruption of fiber tracts before the overall diffusion rate is changed.

The goal of this article is to review the basic principles of full-tensor diffusion-weighted MRI and its clinical application in cerebral ischemia and traumatic brain injury.

## Technical principles of DWI

In the most typical approach of DWI, the MRI sequences are made sensitive to molecular diffusion by adding two extra gradient pulses that are located symmetrically before and after the 180° refocusing pulse. This pair of gradient pulses was first added to a standard spin-echo (SE) sequence in 1965 by Stejskal and Tanner [1]. The physical principle behind DWI is analogous to that of phase-contrast MR angiography (MRA). The first gradient pulse causes molecules to acquire phase shifts, the second gradient pulse will cancel the phase shifts by rephasing the (stationary) spins. Moving spins will, however, acquire a phase shift (incomplete rephasing) due to their motion. This dephasing results in an MR signal loss. As water diffusion is random, the resulting phase

shifts accumulated by the water molecules are also random leading to dephasing with substantial signal loss. The degree of signal loss is determined by the degree of random motion (characterized by the diffusion coefficient) and by the strength and duration of the diffusion-encoding gradients. The higher the degree of random motion (e.g. CSF), the larger the degree of signal drop; conversely, the lower the degree of random motion (e.g. corpus callosum, thalamus, basal ganglia, cortex), the lower the degree of resulting signal drop (Fig. 1).

The degree of signal drop can be enhanced by increasing the strength and duration of the diffusion-encoding gradients. This relationship is characterized by the following equation:

$$SD \sim e^{-bD} \quad (1)$$

where SD represents the signal drop, D the diffusion coefficient, and the variable  $b$  depends on the amplitude, duration, and interval of the diffusion-encoding gradients and can be calculated from the Stejskal–Tanner equation:

$$b = \gamma^2 G^2 \delta^2 (\Delta - \delta/3) \quad (2)$$

where  $\gamma$  is the gyromagnetic ratio, and  $G$ ,  $\delta$ , and  $\Delta$  correspond to the amplitude, duration, and interval of the gradients.

As the DWI sequences rest upon a T2-weighted sequence, the signal intensity of a voxel of tissue is equal to the signal intensity on a T2-weighted image (or  $b \approx 0$  s/mm<sup>2</sup>) decreased by an amount of signal drop related to the diffusion coefficient and the applied  $b$  value. The resulting signal intensity (SI) can be calculated as follows:

$$SI = SI_0 \times e^{-bD} \quad (3)$$

where  $SI_0$  is the signal intensity on the T2-weighted image (or  $b \approx 0$  s/mm<sup>2</sup>).

In clinical practice, images are generally acquired with a  $b$  value of 1000 s/mm<sup>2</sup>. The diffusion-weighted images have shown their greatest clinical utility to date in the identification of abnormal diffusion as encountered in acute cerebral ischemia. The area of restricted diffusion is identified as an area of signal increase against a hypointense background (Fig. 2).

Maps of diffusion rates are calculated by measuring at least two image sets with different  $b$  values: one with a low  $b$  value ( $b$  near to zero) and one with a high  $b$  value (typically  $b=1000$  s/mm<sup>2</sup>). By plotting the  $\ln$  of the measured signal intensity vs the  $b$  values, the diffusion rate can be derived from the slope of this plot. The rate of diffusion is measured in units of area divided by time (e.g. square millimeters per second). The observed diffusion of molecules within biological environments is determined by a variety of known and unknown factors. This includes the previously mentioned microenvironmental architecture but also energy dependent transport

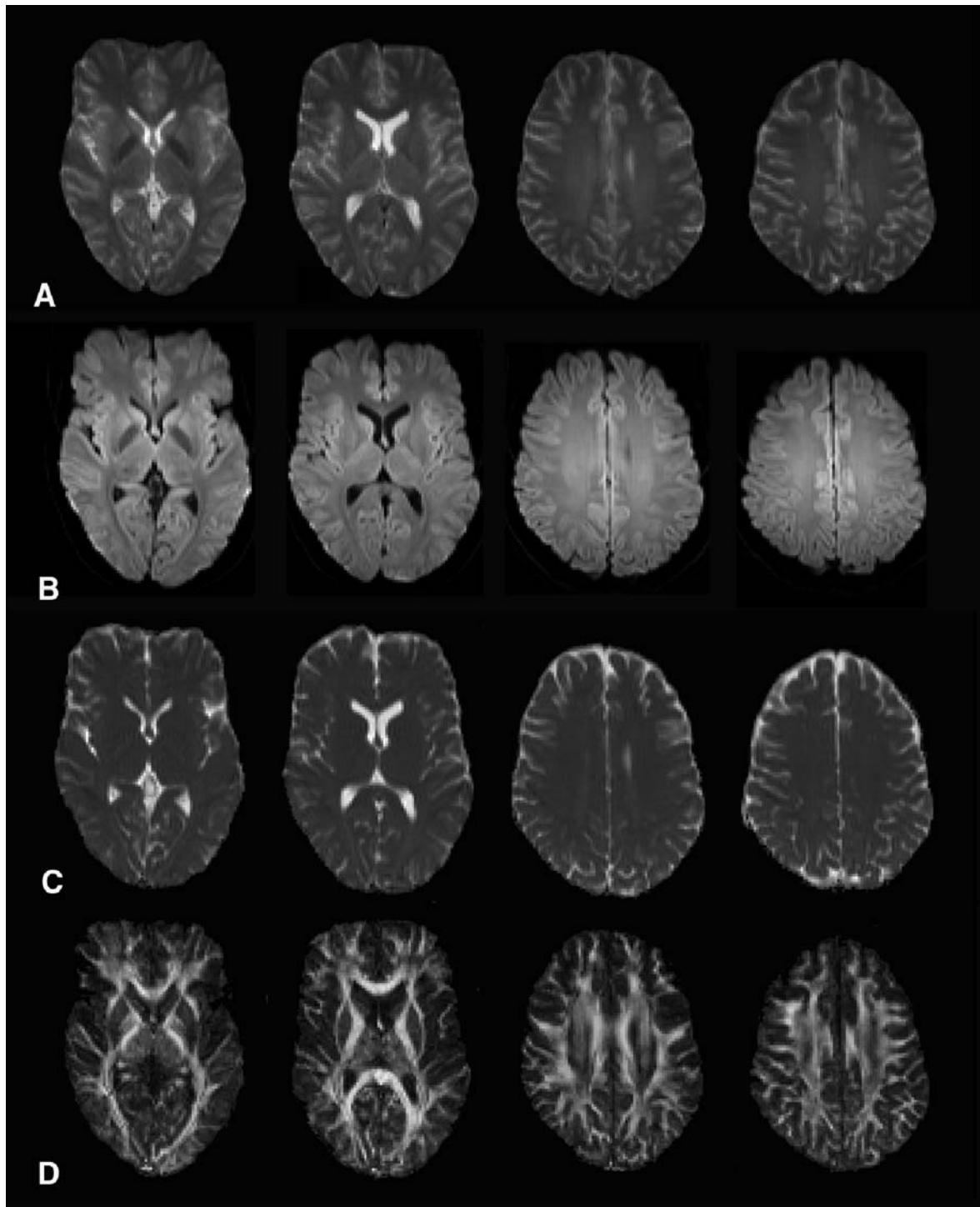


**Fig. 1** Full tensor diffusion data set with reconstruction of **A** low- $b$  images, **B** isotropic diffusion-weighted imaging (DWI) images, **C** apparent diffusion coefficient (ADC) maps, and **D** fractional anisotropy (FA) maps. The low- $b$  images are essentially T2-weighted. The isotropic DWI images show a clear gray–white matter

contrast, whereas the signal intensity is homogeneous on the ADC maps because the ADC values of the gray and white matter are similar. The FA images show a high degree of anisotropic diffusion (hyperintense) along the white matter tracts, whereas the central and cortical gray matter show a low degree of anisotropy (hypointense)

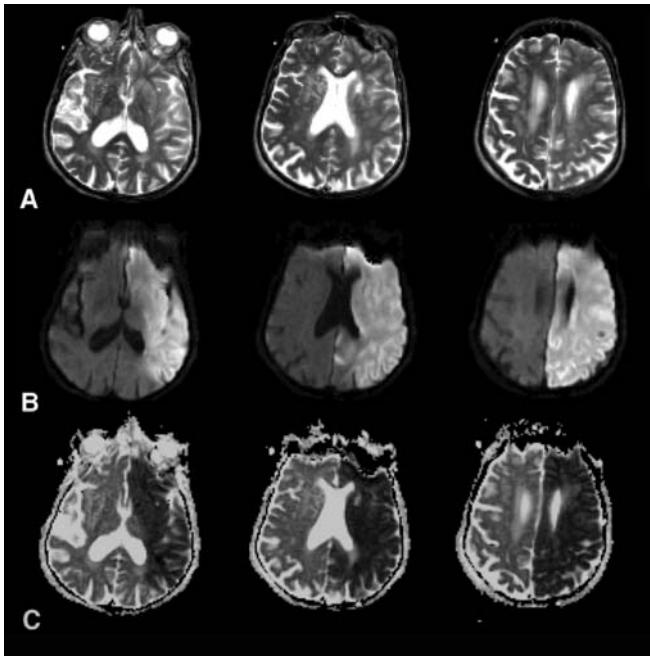


**Fig. 2A–C** An 80-year-old woman with acute right-sided hemiplegia. Imaging reveals the characteristic signal intensities of an acute left-sided ischemia. **A** The ischemic brain tissue is only faintly T2 hyperintense, whereas **B** it is markedly hyperintense on isotropic DWI images. **C** The low ADC values indicate restricted diffusion

tation mechanisms that enhance the motion of water molecules across cell membranes. To respect this variety of factors that influence the measured diffusion, the rate of diffusion in living systems is referred to as the apparent diffusion coefficient (ADC). The ADC values of the single voxels can be displayed as an ADC map revealing the spatial distribution of the different ADC values within a slice of brain tissue (Fig. 1). Areas with a high diffusion will have a high ADC value and appear consequently hyperintense on the ADC maps (e.g. CSF). Areas with restricted diffusion, like areas with acute ischemia, will appear hypointense (Fig. 2). Advantage of this representation is the independence of the signal intensity to T2 phenomena or to the magnetic field strength and gradient strength. The ADC value is an absolute quantitative measurement of translational water motion, which can be compared in serial examinations.

On most commercial MRI scanners, DWI gradient pulses are applied in at least three orthogonal sampling directions as diffusion within the brain, especially within the white matter, has a strong directional preponderance. As mentioned previously, diffusion within the white matter is not isotropic but anisotropic [7, 8]. The exact causes of the anisotropic features of the white matter are not yet completely understood, but most investigators believe that the myelin sheaths play a contributory role, enhancing the diffusion of water molecules along the ax-

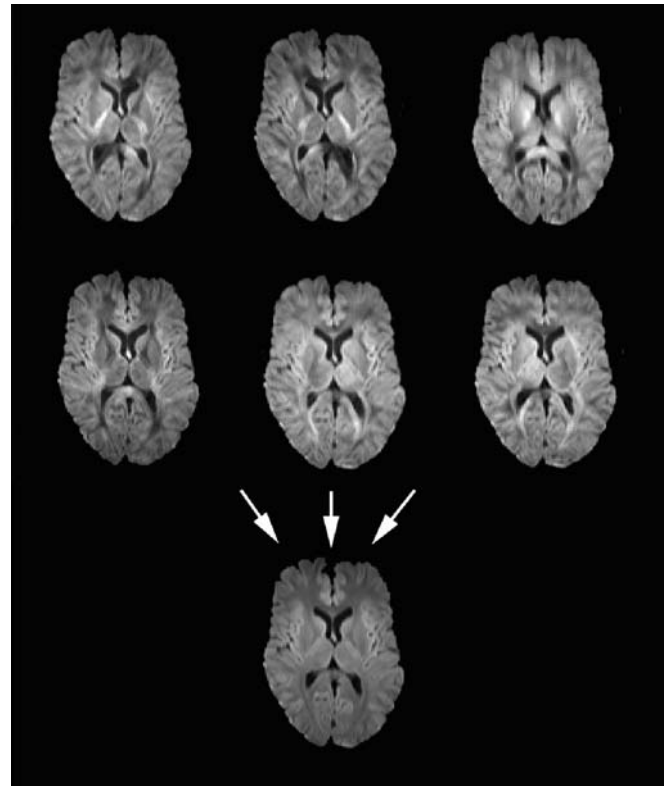


**Fig. 3** Diffusion-weighted images with six different axes of diffusion sensitizing gradients (*top and middle rows*). The DWIs have different contrast depending on the anisotropic nature of diffusion in the brain and the direction of the applied diffusion gradients. The diffusion gradients in this example were sequentially played out in a 1:1:0 ratios: the used order of the diffusion sensitivities was [1,1,0], [1,-1,0], [0,1,1], [0,-1,1], [1,0,1], and [-1,0-1]. White matter tracts parallel to the diffusion-sensitizing gradient appear hypointense, whereas white matter tracts perpendicular to the diffusion sensitizing gradient are relatively hyperintense because of their restricted diffusion in that direction. The isotropic DWI (*bottom row*) is calculated from the previous images (*arrows*). The signal-to-noise ratio (SNR) is consequently improved by signal averaging. In addition, the anisotropic components are cancelled out

is of myelinated white matter tracts, whereas the diffusion across the myeline sheaths is restricted. In addition to the axonal direction and myelination, physiological processes, such as axolemmic flow, extracellular bulk flow, capillary blood flow, and intracellular streaming, may also contribute to white matter anisotropy [9, 10]. Anisotropy can become apparent in clinical practice as diffusion gradients are typically applied in only one geometric direction at a time. On these individual images, diffusion can appear either increased or restricted depending on the geometric relation between the applied diffusion gradients and predominant course of the fiber tracts. The anisotropic nature of diffusion within the brain can be appreciated by evaluating the individual DWI images (Fig. 3). Each image represents information about the direction and magnitude of the diffusion. Be-



cause the hyperintensities due to anisotropy can mimic pathology, most clinical imaging is performed by using methods to reduce these anisotropy artifacts. The simplest way to do this is by acquiring multiple images, each with different gradient-encoding directions (along three orthogonal directions: x, y, and z axes), and then averaging the images (Fig. 3).

By sampling the diffusion in at least three orthogonal directions the “trace” or average of the diffusion can be appreciated. The trace represents the average ADC in all three principal directions and is related to the magnitude of the ADC rather than the directionality of the ADC. The resulting DWI image is described as the isotropic DWI image (Fig. 3). The signal intensity of the isotropic DWI image is essentially the cube root of the multiplied signal intensities of the three individual images acquired with a diffusion gradient in each of the three orthogonal directions. The isotropic DWI image also incorporates T2 contrast.

For clinical evaluation of brain injury in addition to conventional MRI sequences, isotropic DWI images and ADC maps are calculated and studied.

### Advances in diffusion-weighted MRI

There are ongoing advances in the theory and practice of DWI. Some of these advances are progressively introduced in routine imaging. These advances are too numerous and technical to describe in detail here, but a brief mention of a few of these techniques may be appropriate.

One area of active pursuit represents the analysis of the shape of the full diffusion tensor (diffusion tensor imaging, DTI) rather than simply the mean, or trace, of the tensor. The diffusion tensor is a 3D data set in which each element in the tensor has an associated magnitude and direction of diffusion. The diffusion tensor of white matter tracts should be considered as a 3D structure with three principal diffusivities (eigen values) associated with three mutually perpendicular principal directions (eigen vectors). While the trace-weighted images, the signal intensity of which is equal to the magnitude of diffusion, are currently used in clinical practice, there is now evidence that suggests that the shape of the diffusion tensor may change independently from the overall size or magnitude of the diffusion tensor [8, 11, 12, 13]. The shape has been quantified through the calculation of one of a variety of scalar metrics. The most widespread appears to be the calculation of fractional anisotropy. Fractional anisotropy (FA) is defined as the ratio of the anisotropic component of the diffusion tensor to the whole diffusion tensor [11]. The FA has been reported to be the best rotationally invariant scalar metric for measuring diffusion anisotropy [11]. The FA metrics are scalar indices ranging from 0 to 1. Zero represents maximal

isotropic diffusion as in a perfect sphere. One represents maximal anisotropic diffusion as in the hypothetical case of a long cylinder of minimal diameter. While there are only preliminary results, it appears that the fractional anisotropy decreases in subacute and chronic stroke, suggesting tissue breakdown and increased disorganization in the infarcted voxels, consistent with breakdown of the cellular microstructure. Intriguingly, however, there are data that suggest that fractional anisotropy may increase in hyperacute and acute stroke [14]. The pathophysiological mechanisms and full implications of this are not yet understood.

Prerequisite for diffusion-tensor imaging (DTI) is that the entire diffusion tensor is sampled. The tensor has three degrees of freedom and is represented by a 3×3 symmetric matrix ( $D_{xx}, D_{xy}, D_{xz}, D_{yx}, D_{yy}, D_{yz}, D_{zx}, D_{zy}, D_{zz}$ ). The tensor is sampled for a high b value by using a diffusion-weighted sequence repeated in six different directions instead of nine because  $D_{xy}=D_{yx}$ ,  $D_{xz}=D_{zx}$  and  $D_{yz}=D_{zy}$ . A seventh measurement is performed with a low b value. These seven measurements are the minimum required for solving for the diffusion coefficients that characterize the diffusion tensor. The FA maps are displayed as gray-scale maps. Areas with high degrees of FA are bright (e.g. corpus callosum), areas with low degrees of FA are dark (e.g. gray matter; Fig. 1).

In addition, the spatial direction of the mean anisotropic diffusion gradient within each voxel can be displayed graphically by adding a color coding to the FA maps (Fig. 4). Red indicates a predominant left–right, green an anterior–posterior, and blue a superior–inferior anisotropic diffusion gradient. This color coding can help to display selective injury of fiber tracts running in predominantly one direction [15, 16].

Another area of active pursuit is that of very high b values. While in clinical practice a b value of 1000 s/mm<sup>2</sup> has been widely used with good success, some investigators believe there may be additional value at higher b values. This additional value will probably not be in lesion conspicuity. In fact, there is probably lower lesion conspicuity due to increased gray–white ADC differences at higher b values and much lower signal-to-noise ratio (SNR) [17, 18]. As the b value increases, ADC values decrease in both gray and white matter (Fig. 5). Furthermore, the ADC of the white matter decreases more than that of the gray matter. As a result, an increasing white matter vs gray matter differentiation is seen on the ADC maps with increasing b values [17]. In addition, the white matter becomes brighter than the gray matter on the isotropic DWI images. Quantitative analysis has shown that these changes were due to nonmono-exponential diffusion signal decay of the brain tissue, which is more prominent in white matter than in gray matter [17]. The FA values are not affected by changes in the b values [17]. The use of very high b values

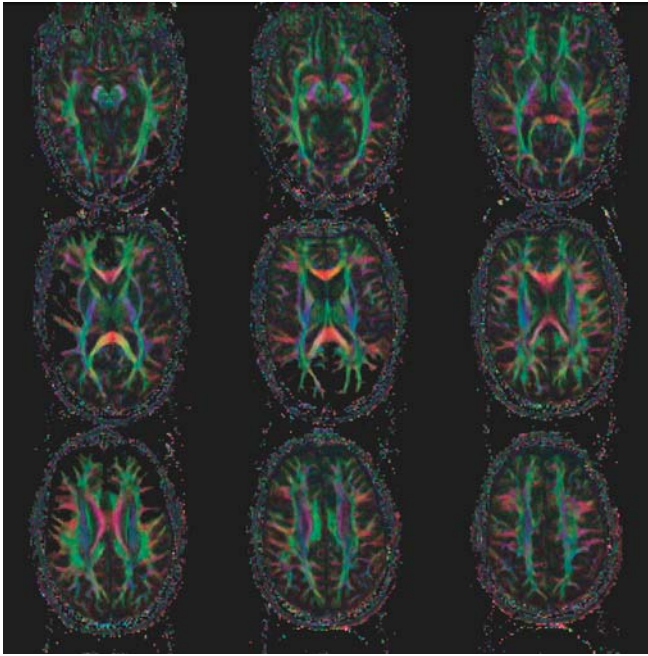


**Fig. 4** Color-coded maps derived from diffusion tensor imaging. Brightness represents the degree of anisotropy and color represents fiber orientation (*red*: left–right; *green*: anterior–posterior; *blue*: superior–inferior). The descending (*blue coded*) fibers of the corticospinal tracts can be followed from the cortex, through the centrum semiovale, internal capsula, and brain stem. The fibers within the genu and splenium corpus callosum that run predominantly from left to right, and vice versa, are red coded

(>3000 s/mm<sup>2</sup>) may, however, shed light on different portions of the cellular anatomy and therefore may provide new insight into stroke pathophysiology.

Finally, it appears clear that the assumption that a single tensor can describe the diffusion of water in a voxel is inadequate, particularly in areas of crossing white matter fiber tracts [15, 16]. The presence of multiple fibers is likely to require more advanced diffusion measurement techniques, which in turn may eventually result in implications for the diagnosis and management particularly of white-matter injury. Supertensor DWI with the acquisition of up to 126 vertices of a fivefold tessellated icosahedron will allow to resolve crossing fiber tracts, eventually resulting in tractography techniques.

## T2 shine-through phenomena

Because the ADC values of gray and white matter are similar, there is typically no contrast between the gray and white matter on ADC maps (Fig. 1). The signal intensity of the gray matter is, however, higher than that of the white matter on isotropic DWI images (Fig. 1). This results from residual T2 contrast on the isotropic DWI images. It is important to understand that the DWI imag-

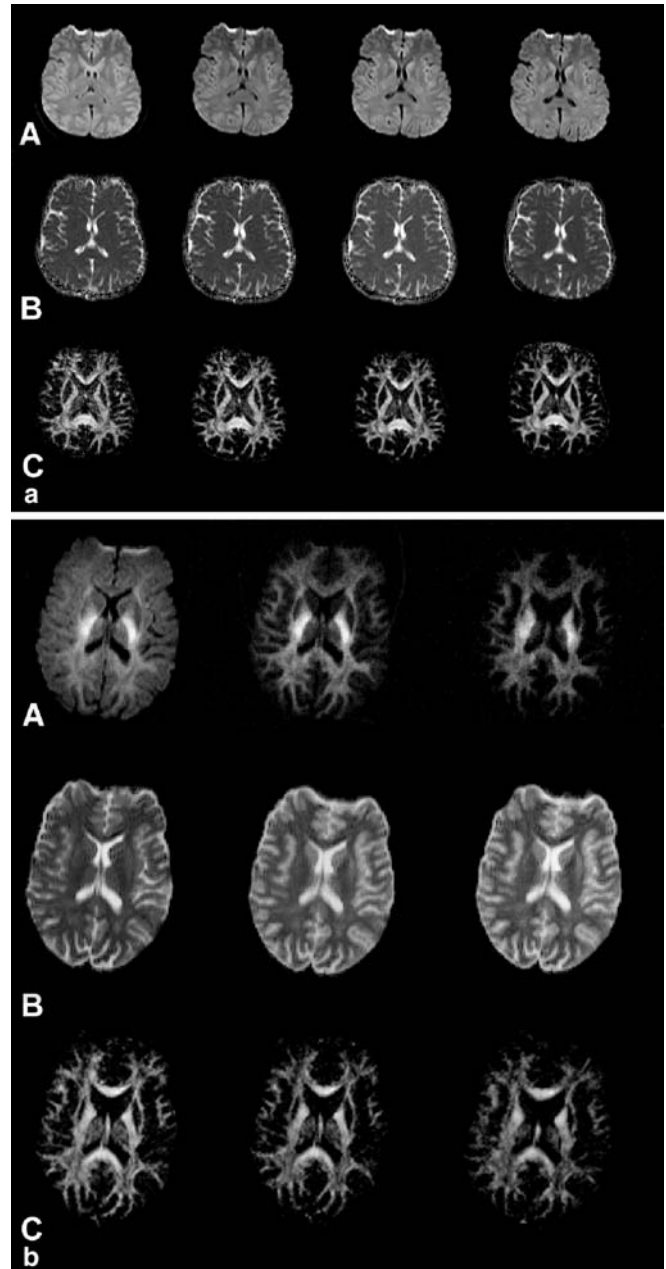


**Fig. 5a, b** Display of isotropic DWI images (A), ADC maps (B), and FA maps (C) that have been measured with different b-values ( $b=300, 500, 700, 1000, 3000, 5000,$  and  $7000$  s/mm<sup>2</sup>). Note the changes of gray–white matter contrast in relation to the increasing b-value in the isotropic DWI images and the corresponding ADC maps. The image contrast on the FA images does not change with the b-values. The SNR decreases with increasing b-values

es have residual T2 contrast and that this can mimic lesions on DWI images. Consequently, it is important to view the ADC maps to differentiate between a lesion with restricted diffusion and a T2 shine-through phenomenon (Fig. 6).

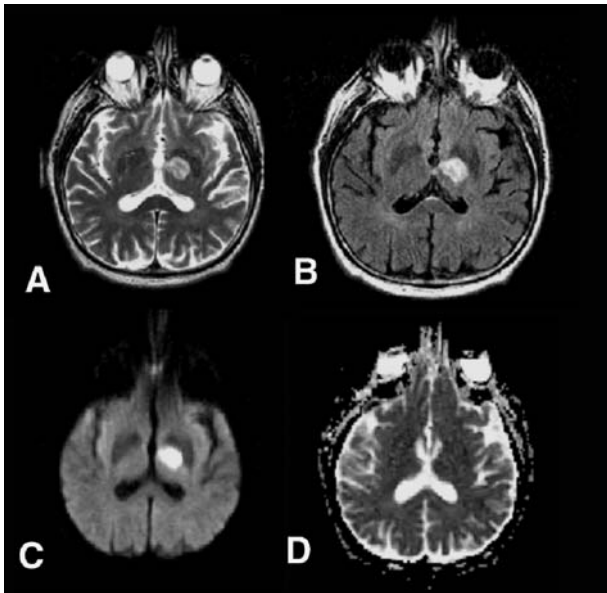


**Fig. 6A–D** “T2 shine-through effect” displayed in a subacute left thalamic infarction. **A** The lesion is hyperintense on T2-weighted fast-spin-echo (FSE) sequence as well as on **B** the fluid-attenuated inversion-recovery (FLAIR) sequence. **C** The lesion appears DWI hyperintense due to the “T2-shine through effect” which is confirmed by **D** the absence of a signal abnormality on the ADC map

### Misregistration artifacts

Misregistration artifacts will affect the spatial resolution and accuracy of the calculated diffusion and anisotropy parameter (Fig. 7). Misregistration results from geometric distortions and misalignment by small motion between the sampled images. The short acquisition times of single-shot echo-planar DWI sequences usually effectively freeze motion artifacts. Geometric distortions can result from static field inhomogeneity due to imperfect shimming, by differences in magnetic properties between adjacent tissues (especially at the skull base) and can result from diffusion sensitization gradient-induced eddy currents. The static field inhomogeneity can be corrected by unwarping algorithms using inhomogeneity field maps. The eddy-current artifacts can be reduced by using a bipolar design of the applied diffusion gradients. Eddy-current artifacts from pairs of positive and negative transitions cancel each other out. Reese et al. showed that misregistration artifacts due to eddy currents are consequently negligible without any calibration and/or correction of diffusion images [19]. In addition, various postprocessing algorithms can partially compensate for these misregistrations.

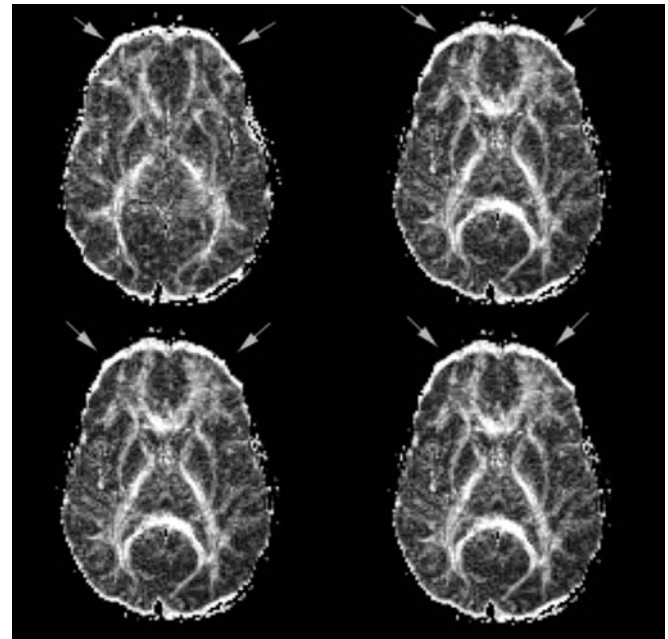


**Fig. 7** Eddy-current-induced image warping of the elementary diffusion tensor images produces geometric distortions that depend on the strength and orientation of the applied diffusion sensitizing gradients. The misregistration can produce severe artifacts. These artifacts are especially apparent on FA maps as a bright rim surrounding the brain (*arrows*). In addition, the boundaries of white matter tracts can be blurred

### Signal-to-noise ratio

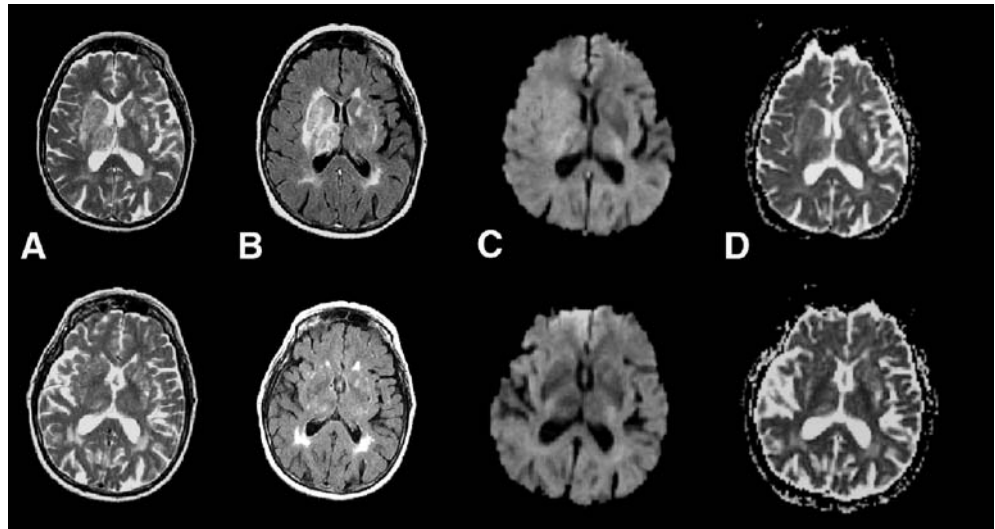
Measurements of diffusion anisotropy are known to be highly noise dependent, especially in areas of low anisotropy where the relation between the sizes of the eigen values of the diffusion tensor to the background noise is less favorable [11, 13, 20, 21]. Consequently, the imaging parameter should be optimized for an adequate SNR. Increasing b values decrease SNR, and higher field strengths increase SNR.

### Clinical application of diffusion-weighted MRI

To date, the most important clinical application of DWI is focused on the early identification of cerebral stroke. Most reports suggest that DWI is able to visualize changes in diffusion rate and shape within minutes after the onset of ischemia [3, 4, 5, 6, 22, 23, 24]. This allows an evaluation of the extent of ischemia in a time frame where possible interventions (e.g. revascularization, thrombolytic agents, tPA) or the use of neuroprotective agents could limit or prevent further brain injury or possibly even reverse brain injury. This is of essential importance as conventional spin-echo MR sequences and conventional CT does not reliably detect infarction with-



**Fig. 8A–D** A 66-year-old woman with deep venous thrombosis. **A** The initial MR examination (*top row*) shows extensive T2 FSE and **B** FLAIR hyperintense signal changes within the central gray and white matter. The lesions are **C** DWI- and **D** ADC hyperintense indicating increased diffusion. These signal changes most likely represent potentially reversible vasogenic edema due to venous stasis, instead of irreversible infarction. Follow-up imaging after 2 months (*bottom row*) shows that most signal changes were indeed reversible



in the first hours after stroke onset. Several studies have reported a limited sensitivity for ischemia within 6 h after stroke onset between 38 and 45% for CT and between 18 and 46% for conventional MR imaging [4, 25]. With an increasing time delay between onset of stroke and imaging the sensitivity consequently increases. Lövblad et al. reported an increased sensitivity of 58% for CT and 82% for MR imaging when examined at 24 h [5]. The sensitivity of DWI is, however, reported to be substantially higher with a sensitivity between 88 and 100% and a specificity between 86 and 100% for acute and hyperacute ischemia underlining the importance of this technique [4, 5, 26]. Next to the early positive identification of ischemia, a negative imaging, excluding ischemia, can often be equally important to the clinicians, as acute stroke is included in the differential diagnosis of almost any neurological process that manifests with sudden neurological deficits. Cerebral venous thrombosis with stasis of blood flow and possible venous stroke can, for example, mimic arterial stroke. The pathophysiological mechanisms and final outcome are, however, essentially different. In venous stroke a considerably larger component of vasogenic (potentially reversible) edema (Fig. 8) develops rather than cytotoxic edema [27, 28, 29]. The neurological deficits can, however, be very similar. In other words, diffusion imaging appears to be of value in the management of patients with suspected acute cerebral ischemia both because of its sensitivity and its specificity.

The pathophysiological basis for the diffusion changes in acute ischemia is not yet completely understood. One widely accepted theory for the restriction of water diffusion in acute stroke relies on a disruption of the energy metabolism with consecutive cellular retention of water, termed cytotoxic edema. The reduced concentration of the main intracellular energy metabolite, adeno-

sine triphosphate (ATP), will result in a failure of the  $\text{Na}^+/\text{K}^+$  and  $\text{Ca}^{2+}$  membrane pumps. The resulting disruption of the ion-homeostasis induces a shift from water from the extracellular to the intracellular space with cellular swelling (cytotoxic edema). Other investigators believe that the predominant reason for the decrease in the diffusion of free water within the cells is due to a direct lack of energy, and only secondarily due to the reduction of the extracellular space by the cellular swelling [30]. In addition, multiple other factors are thought to contribute to the reduced mobility of free water including an increased tortuosity of the extracellular and intracellular space and an increased intracellular viscosity [30]. While there is still active investigation in this area, fortunately for the basic understanding of the clinical application and value of diffusion-weighted MR imaging in acute stroke, the exact mechanisms need not be completely resolved. Instead, a reasonable (over)simplifying hypothesis is that cytotoxic edema occurs early in ischemia and results in a reduction of diffusion. This reduction in diffusion can be identified as an area of hyperintensity on isotropic DWI images and a corresponding hypointensity (reduced ADC values) on ADC maps (Fig. 9). In the appropriate clinical setting the combination of hyperintensity on DWI images and a normal signal on T2-weighted images is pathognomonic for acute stroke. Only acute ischemia can produce cytotoxic edema so rapidly without concomitant vasogenic edema that T2-weighted images remain without signal alterations.

The diffusion signal characteristics of acutely damaged tissue have been shown to follow a temporal evolution paralleling the neuropathological progression of infarcted brain tissue (Fig. 10) [7, 23, 31]. The ADC values decrease within the first few minutes of ischemic insult, usually reaching a minimum ADC value at 8–32 h. The ADC will remain reduced for 3–5 days. On



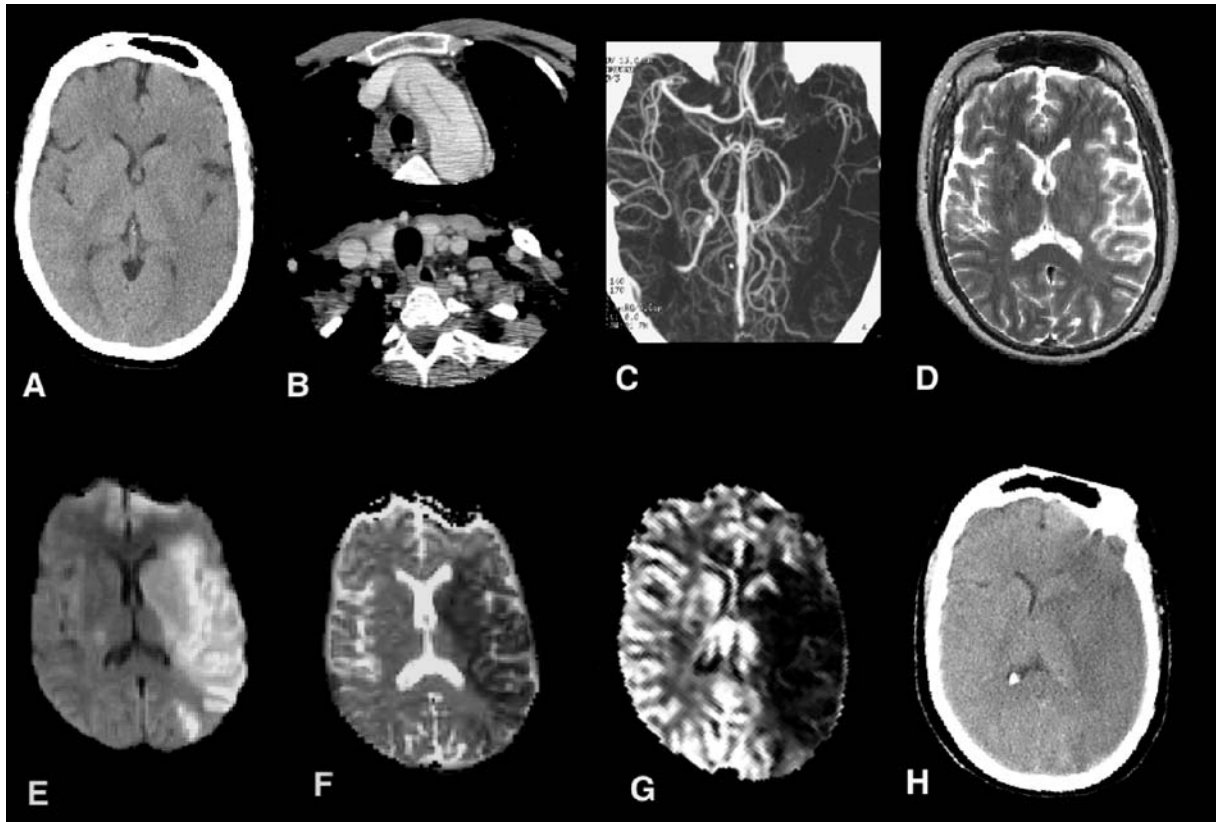


**Fig. 9A–H** Acute left middle cerebral artery (MCA) ischemia in a 45-year-old woman who presented with acute onset of lethargy, aphasia, and right-sided weakness. **A** Acute CT shows a faint hypodensity within the distribution of the left MCA. **B, C** Angio-CT reveals an aortic dissection with extension into the left internal carotid artery and occlusion of the left MCA. **D** The left-sided ischemia can barely be identified by T2 FSE. The ischemia is well depicted on DWI and presents with the characteristic **E** DWI hyperintensity and **F** ADC hypointensity indicating acute ischemia with restricted diffusion (cytotoxic edema). **G** Perfusion-weighted MRI shows a matching area of hypoperfusion. **H** Follow-up CT confirms the acute findings with progressive hypodensity of the ischemic brain tissue

T2-weighted images the lesion will slowly appear as a hyperintense lesion due to the increasing amount of vasogenic edema. Because the signal intensity on DWI has both T2-weighting as well as diffusion weighting, the progressive T2 hyperintensity will raise the conspicuity of the lesion on DWI. After approximately 1 week, the ADC value will slowly return to baseline as the injured cell membranes start to disintegrate, thereby reducing the amount of cytotoxic edema [32]. During this period a “pseudonormalization” will be encountered on the ADC maps. Eventually, the ADC values will start to increase significantly above the baseline, presumably reflecting the progressive tissue resorption and cavitation. On DWI images the lesion will appear hypo-, iso-, or hyperintense depending on the balance between the T2- and diffusion components. The lesion will be hyper-

intense on T2-weighted sequences. The stereotypical time course of the signal characteristics allows the neuroradiologist to estimate the age of the infarction if the onset of symptoms is uncertain (Fig. 10). Recent studies have also shown the evolution of the ADC within the core of an ischemic stroke varies with patient age or infarct etiology. These studies suggested that older patients have a slower rate of pseudonormalization than younger patients do, that ischemic tissue damage may occur more rapidly in older patients, and that there is a heterogeneity in the time course of ADC changes among patient populations [33].

The evolution of signal changes on DWI and ADC maps allows the visualization and diagnosis of new infarctions within or next to chronic infarctions (Fig. 11). This can be a major clinical advantage, as many patients with cerebrovascular disease will have recurrent infarctions within the course of their disease process. Acute and subacute infarctions can be obscured by chronic infarctions on T2-weighted or fluid-attenuated inversion recovery (FLAIR) sequences. The signal characteristics on DWI make this differentiation easy to perform. Acute infarctions will appear hyperintense on DWI images with reduced ADC values as chronic, old infarctions will usually appear iso- or hypointense on DWI images with increased ADC values (Fig. 11).

Finally, the high contrast-to-noise ratio on diffusion-weighted MR imaging enhances lesion conspicuity

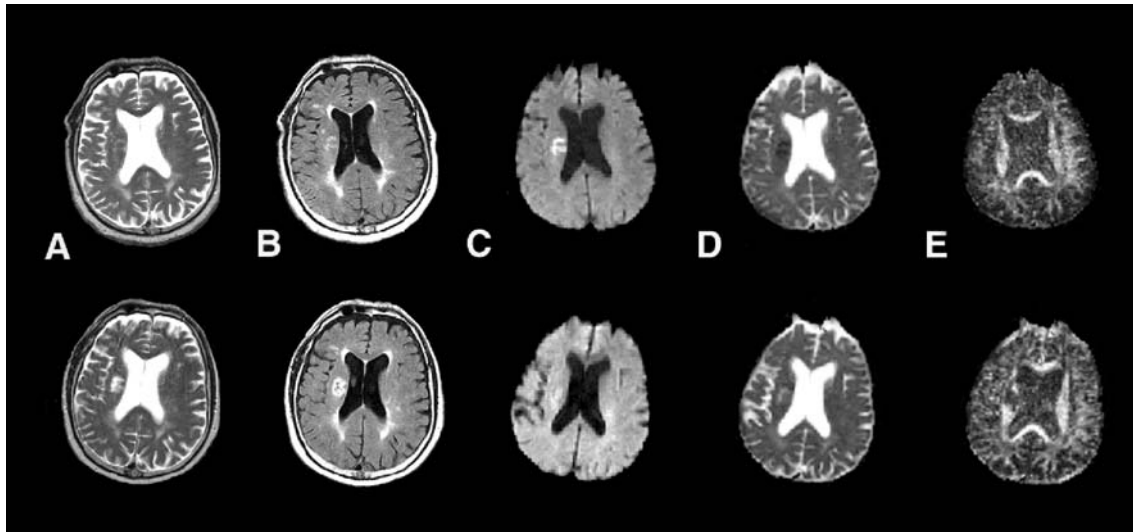


**Fig. 10A–E** Right-sided infarction along the descending white matter tracts: evolution of signal changes over time in a 74-year-old man with dizziness and confusion. The *top row* shows the acute imaging with a mildly **A** T2 FSE and **B** FLAIR hyperintense acute infarction. The lesion is typically **C** DWI hyperintense and **D** ADC hypointense. **E** The FA map does not show any change in anisotropic diffusion. The late follow-up imaging (*bottom row*) shows the characteristic signal changes of a subacute/chronic infarction with a T2 FSE and FLAIR hyperintensity, and a slowly developing ADC hyperintensity indicating cavitation and tissue resolution. The cavitation with disruption of the fiber tracts is confirmed by the FA maps which show a loss of anisotropic diffusion within the lesion

(Fig. 12). An up to 20-fold higher percentage contrast-to-noise ratio on DWI of acute ischemic stroke compared with T2-weighted MRI has been demonstrated [4]. The brightness of an acute infarction against the fairly uniform background on DWI images is especially helpful in the identification of small embolic infarctions (Fig. 12).

It would go beyond the scope of this manuscript to discuss the value of perfusion-weighted imaging (PWI) in cerebral stroke. It is, however, noted that many investigators believe that by correlating DWI findings with PWI findings, tissue at risk for injury within the near and late future can be identified [6, 34, 35]. Multiple studies, dating back to the early 1980s, have described the concept of the “core of an infarction” surrounded by an “ischemic penumbra” [36, 37]. As originally defined, the ischemic penumbra encompasses that portion of oligemic territory where electrical failure has occurred but cellular integrity is maintained [36]. In other words, the cerebral perfusion is believed to be sufficient to keep the neurons alive, but the perfusion is too low to keep the neurons functioning [37]. In the core of the infarction, the perfusion has, however, dropped below the critical threshold where the neurons can survive, and tissue ischemia is usually irreversible [37]. The early identification of the ischemic penumbra with potentially salvageable

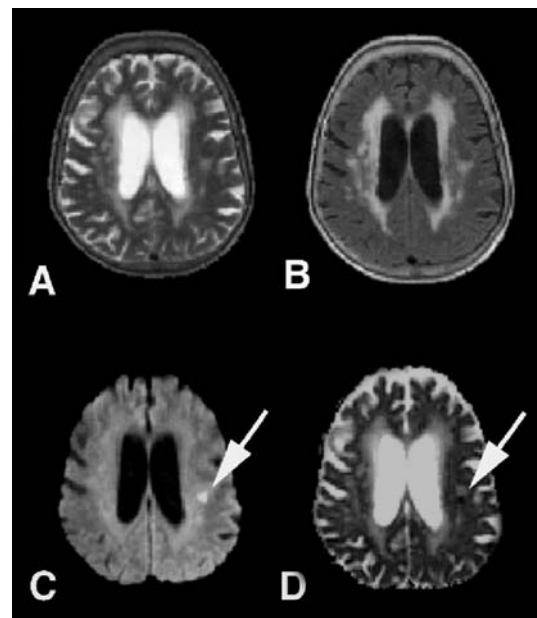


**Fig. 11A–D** An 80-year-old woman with extensive periventricular white matter changes and multiple previous embolic infarctions who presented with an acute neurologic deficit. **A** T2 FSE and **B** FLAIR show the well-known chronic white matter signal changes but cannot identify which lesion is acute/new. **C** Diffusion-weighted imaging clearly shows the small acute embolic infarction with the characteristic DWI hyperintensity combined with **D** an ADC hypointensity (*arrows*)

tissue represents the primary goal of any diagnostic tool. Previous experimental animal stroke studies have shown that the penumbra may remain viable for some time [37, 38, 39, 40, 41, 42]. This offers a time window for therapeutic interventions to salvage tissue at risk for infarct evolution. In human studies viable tissue was found within the ischemic penumbra up to 48 h after stroke onset [38, 39]. It is, however, known that the ischemic pen-

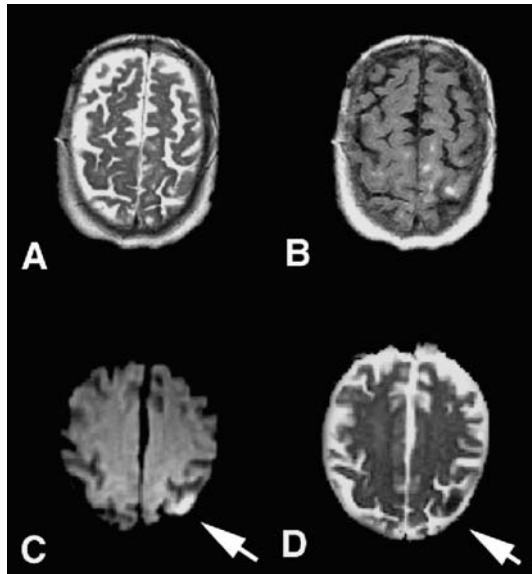


**Fig. 12A–D** An 83-year-old woman with acute right-sided weakness and a previous history of hypertension. Conventional T2 FSE and **A, B** FLAIR imaging show multiple small chronic infarctions. **C** The DWI in combination with **D** the corresponding ADC maps allow localization of the new, acute infarction (*arrows*). In analogy to Figs. 12 and 13, the unique signal features on DWI facilitate the early detection of infarctions

umbra does not remain viable for extended periods of hypoperfusion. Moreover, there is experimental evidence that the cerebral blood flow thresholds to maintain cellular ionic gradients and neuronal integrity increase with increasing duration of the ischemia [40, 43]. Without therapeutic interventions, the initial core of the infarct often gradually expands into the ischemic penumbra [41, 44]. The early identification of the ischemic penumbra is consequently essential in deciding which patients would benefit from a treatment and which would not, in which patients tissue at risk for infarct progression can be salvaged, and in which patients no tissue at risk for infarction progression is present. Schlaug et al. hypothesized that a combination of DWI and PWI studies can be used to define cerebral tissue at risk for infarction in stroke [45]. The DWI is an ideal tool for defining ischemic tissue in the hyperacute stage of human stroke, and areas with reduced ADC values are indicative for the ischemic core of the infarction. PWI can be used to assess the regional blood perfusion and can delineate regions of decreased perfusion that may or may not proceed to infarction. Schlaug et al.'s [45] analysis showed that the ischemic penumbra can operationally be defined by correlating the area of initial diffusion abnormality with the area of hypoperfusion on PWI. Matching areas of DWI and PWI abnormalities were considered as a possible imaging correlate to the core of the infarction (Fig. 13) [6, 34, 35], whereas a DWI/PWI mismatch ( $PWI > DWI$ ) is

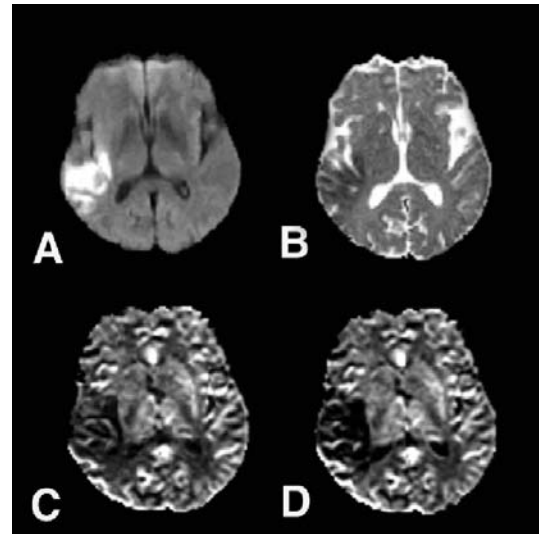


**Fig. 13A–D** A 72-year-old man with acute aphasia and left-sided weakness. **A** Acute DWI hyperintense, and **B** ADC hypointense right MCA infarction. **C** The area of restricted diffusion matches with the area of decreased cerebral blood flow and **D** cerebral blood volume

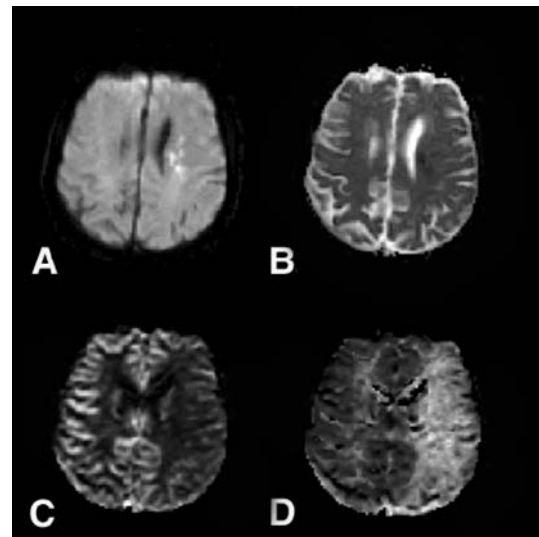


**Fig. 14 A, B** A 68-year-old woman with acute aphasia after thrombendarterectomy of the left MCA shows that multiple small areas of restricted diffusion are seen within the supply of the left MCA. **C** There is a large area of reduced cerebral blood flow and **D** an increased mean transit time that does not match with the diffusion abnormalities indicating tissue at risk for future infarction

considered to correlate with the ischemic penumbra (Figs. 14, 15) [6, 34, 35]. More recent studies extended these results by showing that algorithms combining hyperacute (imaging within 12 h after onset of symptoms) diffusion (T2, ADC, DWI) and perfusion (cerebral blood flow, cerebral blood volume, and mean transit time) data



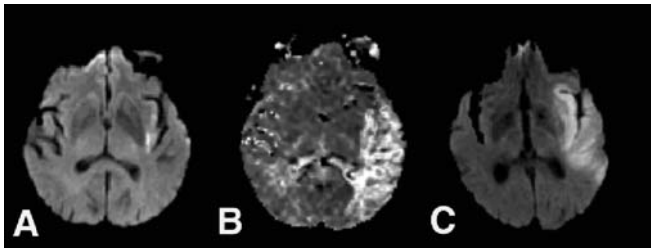


**Fig. 15** Mismatch between **A** initial DWI and **B** Perfusion-weighted imaging with progression of the area of diffusion abnormality on **C** follow-up DWI

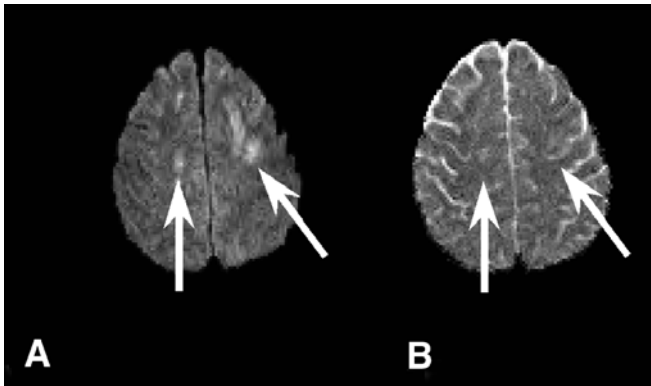


**Fig. 16** Diffuse axonal injury with **A** multiple DWI hyperintense and **B** partially ADC hypointense subcortical shearing injuries (*arrows*) within both hemispheres

can access the risk of infarction with greater sensitivity and specificity than algorithms using diffusion and perfusion data separately [46]. Wu and co-workers showed that thresholding and generalized linear model algorithms combining DWI and PWI data predicted with 66% sensitivity, as well as 83 and 84%, respectively, specificity, voxels that proceeded to infarction [46]. These methods which quantitatively assess the risk of future infarction on a voxel-by-voxel basis do not only guide acute and chronic treatment but can also be used to evaluate efficacy of novel treatments in reducing the risk for future ischemia.

In analogy to stroke-related brain injury, DWI is increasingly investigated for its value in the evaluation of traumatic brain injury [47]. Especially in the evaluation of diffuse axonal injury (DAI), DWI may prove to be valuable (Figs. 16, 17, 18). DAI lesions with increased and decreased diffusion have been observed in traumatic brain injury. One study showed that the majority of the lesions (>67%) show a decreased diffusion [30]. In humans, DAI lesions may be characterized by restricted diffusion as long as 18 days after injury [48]. Smith et al. showed a decreased diffusion within 1 h of injury of moderate severity in a rat brain injury model [49]. Hanstock et al. found that by 4 h following injury of low

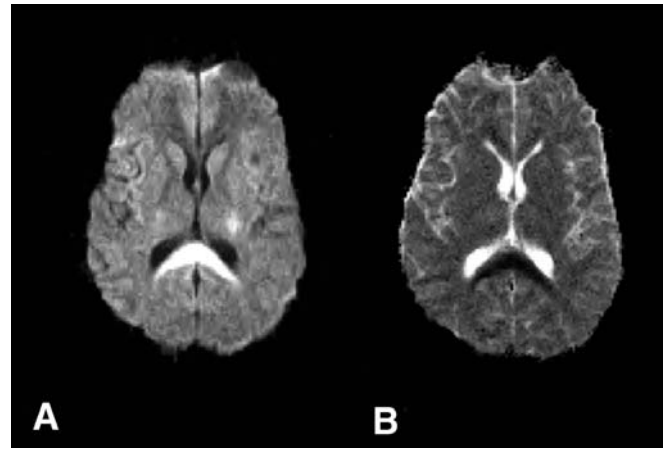


**Fig. 17** Severe shearing injury of the splenium corpus callosum with **A** DWI hyperintensity and **B** ADC hypointensity

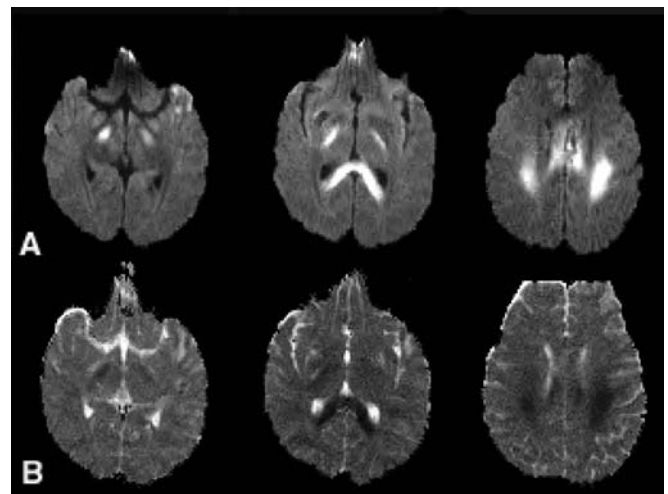


**Fig. 18** Extensive shearing injuries within both hemispheres involving the corticospinal tracts and the splenium and body of the corpus callosum. The lesions are typically **A** DWI hyperintense and **B** ADC hypointense indicating restricted diffusion

severity there appeared to be an increase in the diffusion coefficient in injured cortical and hippocampal tissue, reflecting increased extracellular water [50]. Barzo et al., using an impact acceleration (severe) head-injury animal model, demonstrated a significant increase in ADC during the first 60 min post-injury. This transient increase was followed by a continuing decrease in ADC that began 40–60 min post-injury and reached a minimum value on days 7–14 [51]. Ito et al. [52], who used a similar severe head trauma model as Barzo et al. [51], showed a transient and slight decrease in ADC at 1–3 h after trauma with no significant difference from baseline values when rats were subjected to head injury alone; however, when trauma was coupled with hypotension and hypox-

ia, the ADCs in rat cortex and thalamus decreased significantly and neuronal injury was observed histologically [52]. These findings indicate that lesions with restricted diffusion may be secondary to ischemic and neurotoxic edema.

When lesions with restricted diffusion are encountered in head trauma it is important to assess the lesion location and distribution. Both DAI lesions and ischemic lesions secondary to vascular injury show restricted diffusion. If the lesions are arranged within a vascular distribution rather than at the predilection sites of DAI, a vascular injury should be excluded by additional imaging sequences.

In one of our studies we showed that DWI identifies the largest number of lesions as well as the largest volume of trauma-related signal abnormalities in DAI compared with conventional MRI sequences that include T2-weighted fast-spin-echo, fluid-attenuated inversion recovery and T2\*-weighted gradient-echo sequences [53]. In addition, the total volume of DWI signal abnormalities encountered in DAI demonstrated the highest correlation with acute Glasgow coma scale score and subacute Rankin scale score [54]. These findings indicate that DWI can be a valuable adjunct in the evaluation of DAI in traumatic brain injury.

In another study we showed that in patient with traumatic brain injury, changes in diffusion anisotropy occur within tightly packed white matter tracts (e.g. internal capsula, corpus callosum) [55]. Fractional anisotropy values were significantly reduced within the posterior limb of the internal capsula and within the splenium of the corpus callosum on initial trauma imaging. Furthermore, we found a statistically significant correlation be-

tween these FA values and the severity of head injury as measured by the acute and subacute neurologic assessment tests (acute Glasgow coma scale, Rankin score at discharge from hospital). These results suggest that FA measurements at predilection sites of diffuse axonal injury may serve as a non-invasive biomarker for severity of tissue injury and a possible predictor for later outcome. A major advantage of DTI is that these FA measurements can be performed in a fully sedated or intubated patient in which clinical or neurological examinations cannot assess the patient adequately. The objective, DTI measurements are unlikely to be tainted by the central nervous system side effects of medications or intubation like clinical scores. With further validation, DTI could possibly provide the ability to evaluate responses to treatment when clinical scores are limited to assess the patient's status adequately.

## Appendix

In all presented images (with exception of Fig. 1) full-tensor DWI was performed averaged over three data sets for a total acquisition time of 126 s. The entire diffusion tensor was sampled using a spin-echo single-shot echo-planar sequence repeated in six colinear directions. Imaging parameters were TR=6000 ms, TE=118 ms, slice thickness 6 mm, interslice gap 1 mm, field of view 40×20 cm, and acquisition matrix 256×128 pixels. Diffusion gradients were applied at a finite low b value (3 s/mm<sup>2</sup>) and a high b value (1221 s/mm<sup>2</sup>). The sequence has been previously described in detail [10]. In Fig. 1, images were averaged over eight data sets.

## References

1. Stejskal EO, Tanner JE (1965) Spin diffusion measurements: spin-echo in the presence of a time dependent field gradient. *J Chem Phys* 42:288–229
2. Le Bihan D, Breton E, Lallemand D, Grenier P, Cabanis E, Laval-Jeantet M (1986) MR imaging of intravoxel incoherent motions: application to diffusion and perfusion in neurologic disorders. *Radiology* 161:401–407
3. Provenzale JM, Sorensen AG (1999) Diffusion-weighted MR imaging in acute stroke: theoretic considerations and clinical applications. *Am J Roentgenol* 173:1459–1467
4. Gonzalez RG, Schaefer PW, Buonanno FS, Schwamm LH, Budzik RF, Rordorf G, Wang B, Sorensen AG, Koroshetz WJ (1999) Diffusion-weighted MR imaging: diagnostic accuracy in patients imaged within 6 hours of stroke symptom onset. *Radiology* 210:155–162
5. Lövblad KO, Laubach HJ, Baird AE, Curtin F, Schlaug G, Edelman RR, Warach S (1998) Clinical experience with diffusion-weighted MR in patients with acute stroke. *Am J Neuroradiol* 19:1061–1066
6. Sorensen AG, Buonanno FS, Gonzalez RG, Schwamm LH, Lev MH, Huang-Hellinger FR, Reese TG, Weiskoff RM, Davis TL, Suwanwela N, Can U, Moreira JA, Copen WA, Look RB, Finklestein SP, Rosen BR, Koroshetz WJ (1996) Hyperacute stroke: evaluation with combined multisection diffusion-weighted and hemodynamically weighted echo-planar MR imaging. *Radiology* 199:391–401
7. Sorensen AG, Rosen BR (1996) Functional MRI of the brain. In: Atlas SW (ed) *Magnetic resonance imaging of the brain and spine*. Lippincott-Raven, Philadelphia, pp 1501–1543
8. Pierpaoli C, Jezzard P, Basser PJ, Barnett A, Chiro G di (1996) Diffusion tensor MR imaging of the human brain. *Radiology* 201:637–648
9. Nomura Y, Sakuma H, Takeda K, Tagami T, Okuda Y, Nakagawa T (1994) Diffusional anisotropy of the human brain assessed with diffusion-weighted MR: relation with normal brain development and aging. *Am J Neuroradiol* 15:231–238
10. Wimberger DM, Roberts TP, Barkovich AJ, Prayer LM, Moseley ME, Kucharczyk J (1995) Identification of “premyelination” by diffusion-weighted MRI. *J Comput Assist Tomogr* 19:28–33

11. Sorensen AG, Wu O, Copen WA, Davis TL, Gonzalez RG, Koroshetz WJ, Reese TG, Rosen BR, Wedeen VJ, Weisskoff RM (1999) Human acute cerebral ischemia: detection of changes in water diffusion anisotropy by using MR imaging. *Radiology* 212:785–792
12. Makris N, Worth AJ, Sorensen AG, Papadimitriou GM, Wu O, Reese TG, Wedeen VJ, Davis TJ, Stakes JW, Caviness VS, Kaplan E, Rosen BR, Pandya DN, Kennedz DN (1997) Morphometry of in vivo human white matter association pathways with diffusion-weighted magnetic resonance imaging. *Ann Neurol* 42:951–962
13. Jones DK, Horsfield MA, Simmons A (1999) Optimal strategies for measuring diffusion in anisotropic systems by magnetic resonance imaging. *Magn Reson Med* 42:515–525
14. Wu O, Grant PE, Koroshetz WJ, Gonzalez RG, Rosen BR, Synnott JP, Sorensen AG (2000) Reversal of DWI lesions may be associated with increases in anisotropy (abstr). In: Proc 8th Scientific Meeting of the International Society for Magnetic Resonance in Medicine. Denver, Colorado, p 778
15. Wedeen VJ, Reese TG, Tuch DS, Wiegand MR, Dou JG, Weisskoff RM, Chessler D (2000) Mapping fiber orientation spectra in cerebral white matter with Fourier-transform diffusion MRI (abstr). In: Proc 8th Scientific Meeting of the International Society for Magnetic Resonance in Medicine. Denver, Colorado, p 82
16. Tuch DS, Wedeen VJ, Dale AM, George JS, Belliveau JW (2001) Conductivity tensor mapping of the human brain using diffusion tensor MRI. *Proc Natl Acad Sci USA* 98:11697–11701
17. Yoshiura T, Wu O, Zaheer A, Reese TG, Sorensen AG (2001) Highly diffusion-sensitized MRI of brain: dissociation of gray and white matter. *Magn Reson Med* 45:734–740
18. Meyer JR, Gutierrez A, Mock B, Hebron D, Prager JM, Gorey MT, Homer D (2000) High-b-value diffusion-weighted MR imaging of suspected brain infarction. *Am J Neuroradiol* 21:1821–1829
19. Reese TG, Heid O, Weisskoff RM, Wedeen VJ (1998) Reduction of eddy-current-induced distortion in diffusion MRI using a twice refocused spin echo. *Magn Reson Med* 49:177–182
20. Pierpaoli C, Basser PJ (1996) Toward a quantitative assessment of diffusion anisotropy. *Magn Reson Med* 36:893–906
21. Melhem ER, Itoh R, Jones L, Barker PB (2000) Diffusion tensor MR imaging of the brain: effect of diffusion weighting on trace and anisotropy measurements. *Am J Neuroradiol* 21:1813–1820
22. Chien D, Kwong KK, Gress DR, Buonanno FS, Buxton RB, Rosen BR (1992) MR diffusion imaging of cerebral infarction in humans. *Am J Neuroradiol* 13:1097–1102
23. Warach S, Chien D, Li W, Ronthal M, Edelman RR (1992) Fast magnetic resonance diffusion-weighted imaging of acute human stroke. *Neurology* 42:1717–1723
24. Warach S, Gaa J, Siewert B, Wielopolski P, Edelman RR (1995) Acute human stroke studied by whole brain echo planar diffusion-weighted magnetic resonance imaging. *Ann Neurol* 37:231–241
25. Mohr JP, Biller J, Hilal SK, Yuh WT, Tatemichi TK, Hedges S, Tali E, Nguyen H, Mun I, Adams HP Jr, Grimsman K, Marler JR (1995) Magnetic resonance versus computed tomographic imaging in acute stroke. *Stroke* 26:807–812
26. Marks MP, de Crespigny A, Lentz D, Enzmann DR, Albers GW, Moseley ME (1996) Acute and chronic stroke: navigated spin-echo diffusion-weighted MR imaging. *Radiology* 199:403–408
27. Lovblad KO, Basetti C, Schneider J, Guzman R, El-Koussy M, Remonda L, Schroth G (2001) Diffusion-weighted MR in cerebral venous thrombosis. *Cerebrovasc Dis* 11:169–176
28. Chu K, Kang DW, Yoon BW, Roh JK (2001) Diffusion-weighted magnetic resonance in cerebral venous thrombosis. *Arch Neurol* 58:1569–1576
29. Keller E, Flacke S, Urbach H, Schild HH (1999) Diffusion- and perfusion-weighted magnetic resonance imaging in deep cerebral venous thrombosis. *Stroke* 30:1144–1146
30. Schaefer PW, Grant PE, Gonzalez RG (2000) Diffusion-weighted MR imaging of the brain. *Radiology* 217:331–345
31. Schlaug G, Siewert B, Benfield A, Edelman RR, Warach S (1997) Time course of the apparent diffusion coefficient (ADC) abnormality in human stroke. *Neurology* 49:113–119
32. Matsumoto K, Lo EH, Pierce AR, Wei H, Garrido L, Kowall NW (1995) Role of vasogenic edema and tissue cavitation in ischemic evolution on diffusion-weighted imaging: comparison with multiparameter MR and immunohistochemistry. *Am J Neuroradiol* 16:1107–1115
33. Copen WA, Schwamm LH, Gonzalez RG, Wu O, Harmath CB, Schaefer PW, Koroshetz WJ, Sorensen AG (2001) Ischemic stroke: effects of etiology and patient age on the time course of the core apparent diffusion coefficient. *Radiology* 221:27–34
34. Rordoff G, Koroshetz WJ, Copen WA, Cramer SC, Schaefer PW, Budzik RF Jr, Schwamm LH, Buonanno F, Sorensen AG, Gonzalez G (1998) Regional ischemia and ischemic injury in patients with acute middle cerebral artery stroke as defined by early diffusion-weighted and perfusion-weighted MRI. *Stroke* 29:939–943
35. Schwamm LH, Koroshetz WJ, Sorensen AG, Wang B, Copen WA, Budzik R, Rordorf G, Buonanno FS, Schaefer PW, Gonzalez RG (1998) Time course of lesion development in patients with acute stroke: serial diffusion- and hemodynamic-weighted magnetic resonance imaging. *Stroke* 29:2268–2276
36. Astrup J, Siesjo BK, Symon L (1981) Thresholds in cerebral ischemia: the ischemic penumbra. *Stroke* 12:723–725
37. Symon L (1980) The relationship between CBF, evoked potentials and the clinical features in cerebral ischaemia. *Acta Neurol Scand* 78 (Suppl):175–190
38. Marchal G, Beaudouin V, Rioux P, Sayette V de la, Le Doze F, Viader F, Derlon JM, Baron JC (1996) Prolonged persistence of substantial volumes of potentially viable brain tissue after stroke: a correlative PET–CT study with voxel-based data analysis. *Stroke* 27:599–606
39. Furlan M, Marchal G, Viader F, Derlon JM, Baron JC (1996) Spontaneous neurological recovery after stroke and the fate of the ischemic penumbra. *Ann Neurol* 40:216–226
40. Heiss WD, Graf R, Wienhard K, Lottgen J, Saito R, Fujita T, Rosner G, Wagner R (1994) Dynamic penumbra demonstrated by sequential multitracer PET after middle cerebral artery occlusion in cats. *J Cereb Blood Flow Metab* 14:892–902
41. Heiss WD, Huber M, Fink GR, Herholz K, Pietrzyk U, Wagner R, Wienhard K (1992) Progressive derangement of periinfarct viable tissue in ischemic stroke. *J Cereb Blood Flow Metab* 12:193–203
42. Memezawa H, Smith ML, Siesjo BK (1992) Penumbra tissues salvaged by reperfusion following middle cerebral artery occlusion in rats. *Stroke* 23:552–559



43. Hossmann KA (1995) Viability thresholds and the penumbra of focal ischemia. *Ann Neurol* 36:557–565
44. Quast MJ, Huang NC, Hillman GR, Kent TA (1993) The evolution of acute stroke recorded by multimodal magnetic resonance imaging. *Magn Reson Imaging* 11:465–471
45. Schlaug G, Benfield A, Baird AE, Siewert B, Lovblad KO, Parker RA, Edelman RR, Warach S (1999) The ischemic penumbra: operationally defined by diffusion and perfusion MRI. *Neurology* 53:1528–1537
46. Wu O, Koroshetz WJ, Ostergaard L, Buonanno FS, Copen WA, Gonzalez RG, Rordorf G, Rosen BR, Schwamm LH, Weisskoff RM, Sorensen AG (2001) Predicting tissue outcome in acute human cerebral ischemia using combined diffusion- and perfusion-weighted MR imaging. *Stroke* 32:933–942
47. Hergan K, Schaefer PW, Sorensen AG, Gonzalez RG, Huisman TAGM (2002) Diffusion-weighted MRI in diffuse axonal injury of the brain. *Eur Radiol* 12:2536–2541
48. Liu AY, Maldjian JA, Bagley LJ, Sinson GP, Grossman RI (1999) Traumatic brain imaging: diffusion-weighted MR imaging findings. *Am J Neuroradiol* 20:1636–1641
49. Smith DH, Meaney DF, Lenkinski RE, Alsop DC, Grossman R, Kimura H, McIntosh TK, Gennarelli TA (1995) New magnetic resonance imaging techniques for the evaluation of traumatic brain injury. *J Neurotrauma* 12:573–577
50. Hanstock CC, Faden AI, Bendall RM, Vink R (1994) Diffusion-weighted imaging differentiates ischemic tissue from traumatized tissue. *Stroke* 25:843–848
51. Barzo P, Marmarou A, Fatouros P, Hayasaki K, Corwin F (1997) Contribution of vasogenic and cellular edema to traumatic brain swelling measured by diffusion-weighted imaging. *J Neurosurg* 87:900–907
52. Ito J, Marmarou A, Barzo P, Fatouros P, Corwin F (1996) Characterization of edema by diffusion-weighted imaging in experimental traumatic brain injury. *J Neurosurg* 84:97–103
53. Huisman TAGM, Sorensen AG, Hergan K, Gonzalez RG, Schaefer PW (2003) Diffusion weighted imaging for the evaluation of diffuse axonal injury in closed head injury. *J Comput Assist Tomogr* 27:5–11
54. Schaefer PW, Huisman T, Schwamm LH, Sorensen AG, Halpern EF, Gonzalez RG (2002) Magnetic resonance imaging in diffuse axonal injury: correlation with early Glasgow Coma Scale and Rankin Scale on Discharge (abstr). The 40th Annual Meeting and Symposium of the American Society of Neuroradiology, Vancouver, p 287
55. Huisman TAG, Schaefer PW, Schwamm LH, Ozsunar Y, Hergan K, Wu O, Sorensen AG (2002) Diffusion tensor imaging as biomarker for severity of head trauma (abstr). The 40th Annual Meeting and Symposium of the American Society of Neuroradiology, Vancouver, p 57